Chinese Journal of
POLYMER SCIENCE

RESEARCH ARTICLE

https://doi.org/10.1007/s10118-023-2959-6
Chinese J. Polym. Sci. **2023**, *41*, 1198–1205

Rapid Conversion of Perhydropolysilazane into Thin Silica Coating at Low Temperature

Wen-Yue Wang[a,b], Yu-Lin Zhang[a], Xiang Guo[a], Li-Ming Wang[c,d], Jun-Rong Zhang[c,d], Hui Yang[a], Guo-Jun Dong[b*], Zong-Bo Zhang[a*], and Cai-Hong Xu[a]

[a] *Key Laboratory of Science and Technology on High-tech Polymer Materials, Institute of Chemistry, Chinese Academy of Sciences, Beijing 100190, China*
[b] *Yantai Research Institute, Harbin Engineering University, Yantai 264000, China*
[c] *Institute of High Energy Physics, Chinese Academy of Sciences, Beijing 100049, China*
[d] *Spallation Neutron Source Science Center, Dongguan 523803, China*

Electronic Supplementary Information

Abstract The conversion of perhydropolysilazane (PHPS) to silica at low temperature is beneficial for its application on thermally vulnerable substrates. In this work, it is demonstrated that (3-aminopropyl)triethoxysilane (APTES) has high catalytic efficiency for the low temperature conversion of PHPS and the catalytic mechanism of APTES was suggested. The influence of temperature and humidity on the catalytic conversion process was investigated, and it was found that PHPS can be rapidly converted to silica in 10 min at 80 °C with relative humidity of 90%. The achieved silica is mainly composed of $SiNO_3/SiO_3OH$ and SiO_4 structure with O/Si of 1.74 and N content of 1%. As an approach to prepare inorganic coating, the low-temperature conversion method achieves a silica coating with low volume shrinkage of 0.86%, low roughness of R_a=0.293 nm, high nanoindentation hardness of 3.62 GPa and modulus of 30.06 GPa, which exhibits high potentials as protective coating for various materials even those vulnerable to high temperature.

Keywords Perhydropolysilazane; (3-Aminopropyl)triethoxysilane; Silica coating; Rapid conversion; Catalysis

Citation: Wang, W. Y.; Zhang, Y. L.; Guo, X.; Wang, L. M.; Zhang, J. R.; Yang, H.; Dong, G. J.; Zhang, Z. B.; Xu, C. H. Rapid conversion of perhydropolysilazane into thin silica coating at low temperature. *Chinese J. Polym. Sci.* **2023**, *41*, 1198–1205.

INTRODUCTION

Silica, with excellent optical transparency, insulation, anti-abrasion, chemical inertness and other properties,[1–3] is widely used as the coating material for corrosion prevention,[2] protection,[4] dielectric layers[5–7] and gas barrier coatings.[8–10] To meet the huge demand for applications, mass production through a warm process is highly desired. The main preparation methods of preparing high quality inorganic silica coatings are currently physical vapor deposition,[11,12] chemical vapor deposition,[13–15] atomic layer deposition[14,16] and other vapor deposition techniques. However, the high production cost, harsh production environment and high-vacuum equipment dependence hinder its application. Since 1995, Matsuo *et al.*[17] prepared silica from perhydropolysilazane (PHPS), an inorganic polymer with repeating —Si—NH— unit in its backbone and —H as side groups (Fig. 1a), the method of preparing silica coatings from the convenient and easy scalable solution process has been attracting more and more attention.[18–21]

As reported, PHPS can be converted into highly-dense amorphous silica by high-temperature treatment. Matsuo *et al.*[17] found that dense silicon oxide coating could be obtained after heat treatment of PHPS at 450 °C. Kamiya *et al.*[22] investigated the effect of temperature on PHPS conversion and found that the main reaction involved in the conversion process is the hydrolysis of Si—H and Si—N with the followed condensation of the formed Si—OH to form Si—O—Si. Obviously, the high-temperature process limits the application of PHPS derived silica material. With the development of flexible display, organic photonic voltage and organic LED, more and more thermally sensitive materials, such as poly-

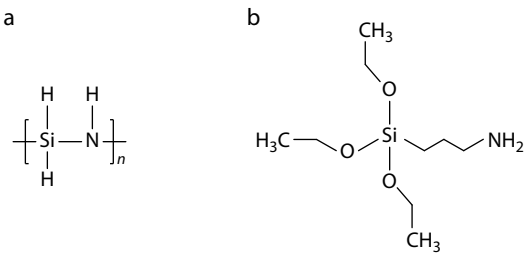

Fig. 1 Chemical structures of (a) PHPS and (b) APTES.

* Corresponding authors, E-mail: dgj1129@163.com (G.J.D.)
E-mail: zongbo@iccas.ac.cn (Z.B.Z.)

Invited Research Article of Special Issue on "The Youth Innovation Promotion Association of the Chinese Academy of Sciences"
Received December 27, 2022; Accepted January 31, 2023; Published online March 17, 2023

mer films and adhesive, which needs silica as gas barrier or electrical insulation layer, are adopted. Thus, low-temperature conversion approach of PHPS to silica is critically demanded. Actually, much effort has been contributed to the investigation of low-temperature conversion for PHPS, which can be divided into two categories, *i.e.* vacuum ultraviolet (VUV) irradiation[5,6,10,18] and catalytic conversion.[23–25] VUV can quickly convert PHPS to dense silica *via* photocleavage-oxidation reaction within minutes at room temperature. However, the method of VUV radiation has relative limited penetration depth due to the absorption of photon by PHPS and oxygen in air, *e.g.*, 200 nm for 172 nm-VUV,[26] which therefore renders this process only suitable for ultrathin coating. Besides, VUV conversion method is not easily scale-up due to the restriction of the irradiation equipment. Therefore, researchers have developed a series of catalytic conversion methods to achieve low-temperature conversion of PHPS. The reported catalytic process also can be divided into two ways: one is to utilize external catalytic environment assistance, for instance, ammonia aqueous atmosphere[4,23,25,27–29] and aqueous hydrogen peroxide solution;[25,30,31] the other is to add catalysis as a component in PHPS.[24,32,33] Apparently, the former is environmentally dependent and difficult to be applied on a large scale. The latter manner is more convenient and easier to be handled. For example, Je *et al*. achieved the fabrication of dielectric material with high-capacitance and good insulating properties from PHPS at 180 °C with 2-dimetylamino-1-propanol (DMAPO) as catalyst.[33] Nevertheless, considering the need for lower conversion temperature, new catalysis is highly expected to promote the conversion from PHPS to silica.

In this work, a catalyst for PHPS conversion, (3-aminopropyl)triethoxysilane (APTES, Fig. 1b) is reported, which can rapidly convert PHPS to silica at low temperature. The effect of temperature and humidity on the catalytic conversion process of PHPS was investigated. By controlling the amount of the catalyst used and humidity, PHPS can be converted into a silica coating within 10 min at 80 °C. The as-formed silica was investigated, and the coating obtained by rapid conversion was characterized by volume shrinkage, refractive index, density, surface morphology, mechanical property and other properties.

EXPERIMENTAL

Preparation and Conversion of PHPS Coating

Different amounts (1 wt%–10 wt% relative to the amount of PHPS) of APTES (≥98%, Innochem, China) were mixed with PHPS *n*-butyl ether solution (20 wt%, synthesized in our laboratory).[19] The mixed solution was stirred at 300 r/min for 4 h at room temperature to ensure homogeneous mixing. The PHPS coating was obtained by spin-coating the solution onto the monocrystalline (100) silicon wafer. The thickness of the coating can be controlled between tens of nanometers and 1 μm by regulating the solution concentration and spin coating speed. Then, silica coating was obtained by converting PHPS in the constant temperature and humidity chamber.

Characterization

The chemical composition and structure of the converted materials were characterized by Fourier transform infrared spectrometry (FTIR), X-ray photoelectron spectroscopy (XPS) and solid-state ^{29}Si-NMR (SS ^{29}Si-NMR). FTIR was measured by the infrared spectrometer (Bruker VERTEX 70v, Germany), and the samples to be measured were prepared on single-crystal silicon (100). The blank monocrystalline silicon wafer was used as the reference for the spectra, the test range was 4000–400 cm^{-1} with 32 scans. XPS measurement was conducted on the multifunctional photoelectron spectrometer (VG ESCALAB 250XI, USA), using the 200 W monochromatic Al K*α* X-ray source for excitation, and the spectrum was calibrated using C1s of exotic contaminated carbon with the binding energy of 284.8 eV as the reference peak. The SS ^{29}Si-NMR was acquired from the NMR spectrometer (Bruker AVANCE 400, Germany).

The thickness and refractive index of samples were measured by Spectroscopic Ellipsometry (J. A. Woollam Alpha-SE, USA), and the data was fitted using the Cauchy model. The volume shrinkage during PHPS conversion was reflected by the thickness change of the coating, and the volume shrinkage rate was calculated as shown in Eq. (1):

$$\eta = (\delta_0 - \delta)/\delta_0 \times 100\% \quad (1)$$

where η is the volume shrinkage, δ_0 is the thickness before conversion, and δ is the thickness after conversion. The quality and the density homogeneity of the coating were examined by the X-ray reflectivity (XRR) technique. The XRR experiment was conducted at 1W1A beamline at Beijing Synchrotron Radiation Facility (BSRF). It was a diffuse X-ray scattering beamline operating at 8.05 and 13.9 keV, with a flux over 1×10^{11} photons/sec and energy resolution of 4.4×10^{-4}. The mechanical property of the samples was determined by the Nano Indenter (Keysight Technologies G200, China) in continuous stiffness mode with the diamond indenter. In order to eliminate the substrate effect, the sample with a thickness of about 1 μm was adopted with an indentation depth of 200 nm, and data with the penetration depth of 100–110 nm was selected for the calculation of hardness and modulus based on the Oliver-Pharr method.[34] The surface morphology and roughness of the samples were determined by atomic force microscope (AFM, Bruker Multimode 8, Germany) in tap mode with a scanning range of 10 μm × 10 μm. The surface and cross-section micromorphologies of the samples were observed by scanning electron microscope (SEM, HITACHI SU-8020, Japan).

RESULTS AND DISCUSSION

Catalytic Effect of APTES on the Conversion of PHPS at Room Temperature

Fig. 2(a) shows the FTIR spectra of the samples with different APTES contents (1 wt%–10 wt%) after 24 h under ambient conditions (20 °C, 40%RH). The FTIR spectrum of PHPS (black line) shows characteristic absorption bands, including 3360 and 1180 cm^{-1} for N—H, 2180 cm^{-1} for Si—H, and 840 cm^{-1} for Si—N. It is well known that in the presence of water, Si—H and Si—N bonds in PHPS firstly react with H_2O to form Si—OH groups, and Si—OH further condenses to form Si—O—Si structure. However, the results of FTIR spectra (gray line) show that the bands of Si—H and Si—N are not significantly weaken after 24 h conversion at room temperature for PHPS, and the appearance of Si—O—Si bands can not be observed, indicating

https://doi.org/10.1007/s10118-023-2959-6

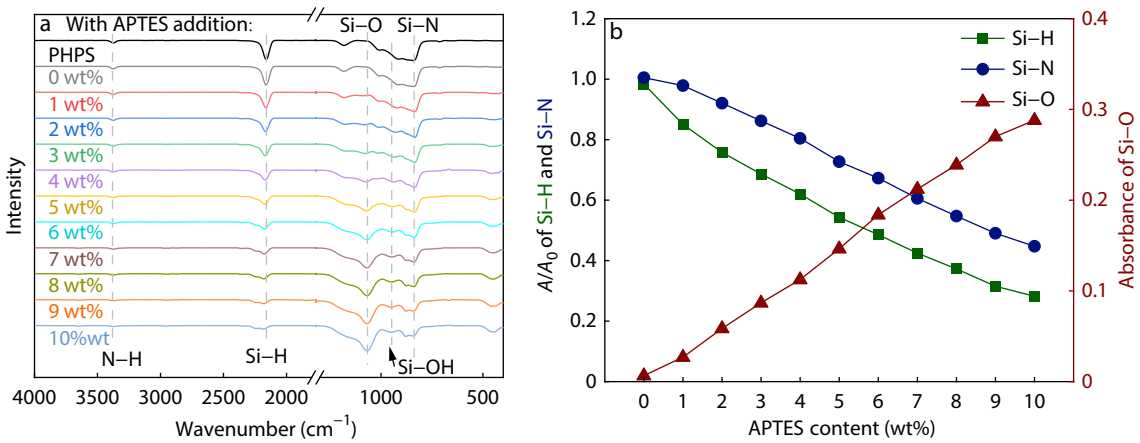

Fig. 2 (a) FTIR spectra of pristine PHPS and PHPS with the addition of different amounts of APTES after 24 h of conversion in room temperature environment (20 °C, 40%RH); (b) The relative absorbance of Si—H and Si—N and the absorbance of Si—O after 24 h conversion at room temperature for PHPS with different APTES content.

that the PHPS without catalysis undergoes almost no conversion to the silica structure at room temperature environment.

In contrast, the addition of APTES greatly promotes the conversion degree of PHPS. The FTIR spectrum shows that the intensity of Si—H and Si—N absorption bands decreases and the band attributed to Si—OH appears at 950 cm^{-1}, indicating that the conversion process is through the hydrolysis of Si—N and Si—H, and the presence of the Si—O absorption band at 1068 cm^{-1} implies further condensation between Si—OH happens. The relative absorbance (A/A_0, A is the absorbance of the samples with different APTES content after 24 h conversion at room temperature, A_0 is the absorbance before conversion) of Si—H and Si—N and the absorbance (A) of the Si—O peak in the FTIR spectra of the samples with different APTES content are compared to investigate the effect of APTES content on the conversion of PHPS (Fig. 2b). It is obvious that after the addition of APTES, the Si—H and Si—N bonds undergo hydrolytic condensation reaction to form Si—O—Si structure. With the increase of APTES content, the conversion degree of PHPS coatings increases and silica becomes the main structure. The above results show that the increase of APTES content in PHPS can accelerate the conversion speed at room temperature.

Scheme 1 exhibits the mechanism of the catalytic conversion of PHPS by APTES. The catalytic effect of APTES on PHPS is mainly reflected in its promotion of the hydrolysis reaction of Si—H and Si—N. In the presence of moisture, the —NH_2 in the APTES structure is hydrolyzed to produce OH^- and —NH_2H^+ intermediates (a). For the Si—H bond, OH^- nucleophilic attack on the Si—H bond generates Si—OH and releases the H^- anion, which combines with the H^+ cation in —NH_2H^+ and produces H_2 (b).[35] For the Si—N bond, under

$$H_2O + —NH_2 \longrightarrow OH^- + —NH_2H^+ \quad (a)$$

$$Si—H + OH^- + —NH_2H^+ \longrightarrow Si—OH + H_2 + —NH_2 \quad (b)$$

$$Si—N + OH^- + —NH_2H^+ \longrightarrow Si—OH + NH_3 + —NH_2 \quad (c)$$

Scheme 1 Suggested mechanism of the catalytic conversion of PHPS by APTES.

the same catalytic mechanism, OH^- attacks the Si—N bond to generate Si—OH and NH_3 (c), and NH_3 can further catalyze the hydrolysis of Si—H and Si—N. Therefore, in the presence of APTES, the Si—H, Si—N hydrolysis reaction in the PHPS is accelerated and more Si-OH groups will be generated, and the increase of Si—OH concentration promotes the production of Si—O—Si. Thus, the acceleration of hydrolysis and condensation reaction facilitates the conversion of the PHPS to the silica structure, which is consistent with the result of FTIR analysis.

Effect of Temperature and Humidity on the Catalytic Conversion Process

To investigate the effect of temperature, the relative humidity was fixed at 40% and the FTIR spectra (Fig. S1a in the electronic supplementary information, ESI) of the coatings were collected after conversion at different temperatures (20–80 °C) for 4 h. The relative absorbance of Si—H and Si—N and the absorbance of Si—O bonds in the FTIR spectra of samples converted at different temperatures are plotted in Fig. 3(a). It is obvious that the conversion rate increases significantly with the increase of temperature, and the conversion rate at 80 °C is three times higher than that at 20 °C according to the change of absorbance of Si—H bond. Since the diffusion coefficient increases with temperature,[36] more water molecules diffuse into PHPS as the temperature rises, and more Si—H and Si—N bonds are hydrolyzed. Meanwhile, the increase in temperature provides the impetus for the condensation reaction, thus, macroscopically the reaction rate increases. The effect of humidity on the catalytic conversion process was investigated using the same method. The temperature was fixed at 20 °C and the FTIR spectra of the coatings were measured after 12 h of conversion at different humidity (40%RH–90%RH) (Fig. S1b in ESI). The variation of absorbance of Si—H, Si—N and Si—O with humidity is shown in Fig. 3(b). The Si—H conversion rate at 90%RH is two times higher than that at 40%RH. Incompletely converted PHPS has high water permeability due to the presence of Si—OH[25] and the water vapor transport is based on a solution diffusion mechanism.[37] Due to the mechanism similar to osmotic pressure, the increase in humidity induces more water molecules to diffuse inside the PHPS coating, which

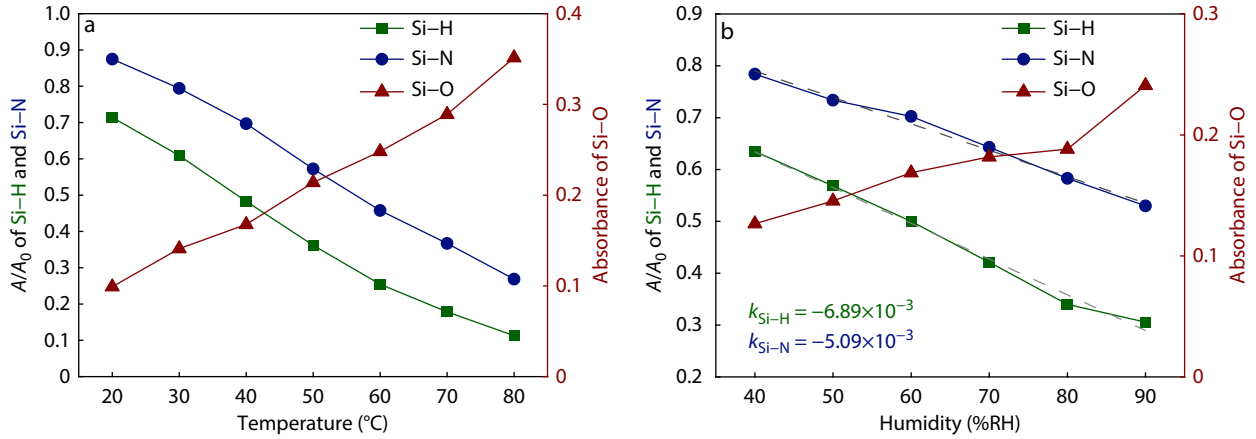

Fig. 3 (a) The relative absorbance of Si—H and Si—N and the absorbance of Si—O of PHPS with 5 wt% APTES after conversion for 4 h at 40%RH at different temperatures; (b) The relative absorbance of Si—H and Si—N and the absorbance of Si—O of PHPS with 5 wt% APTES after conversion for 12 h at 20 °C at different humidity.

enables more Si—H and Si—N undergo hydrolysis reactions, further promotes condensation reactions and the formation of Si—O. By linearly fitting the Si—H and Si—N variation curves in Fig. 3(b), it is found that the Si—H bond changes more rapidly with humidity compared to the Si—N bond ($k_{Si-H}>k_{Si-N}$), indicating that the Si—H in the PHPS is more sensitive to humidity than the Si—N in this catalytic conversion process. The above results show that both temperature and humidity have remarkable influence on the catalytic effect of APTES for conversion of PHPS.

The Conversion of PHPS into the Silica at 80 °C with Relative Humidity of 90%

Considering the conversion rate and the conversion condition, we further investigate the conversion of PHPS to silica at 80 °C with relative humidity of 90%. The FTIR spectra of the samples with different conversion time were measured (Fig. S2 in ESI). It is clearly observed that Si—H and Si—N bonds are rapidly hydrolyzed and condensed to form Si—O bonds within a short period of time (Fig. 4). About 95% of Si—H and 84% of Si—N are consumed in 10 min due to the hydrolysis reaction, indicating that APTES is a highly efficient catalyst to promote the conversion of PHPS to silica coating. The change rate of the Si—H intensity is greater than that of the Si—N, which is similar to the results by changing the humidity. We propose that the dehydrogenation coupling reaction of Si—H[38] (Scheme 2a) occurs and the intermediate Si—NH_2 forms during Si—NH conversion[39] (Scheme 2b).

The XPS analysis of converted material demonstrates a small trace of N element (1%) with O/Si ratio of 1.74 (Fig. 5a, Table S1 in ESI). Based on the presence of a small amount of C element (1.37%), it can be assumed that APTES is present in the sample. Deconvolution of Si 2p peak indicates three peaks at 101.9 eV, 102.9 eV and 103.6 eV, corresponding to —SiH_2NH— (PHPS phase), SiO_x (intermediate phase) and SiO_2 (silica phase),[33,40] respectively. It is obvious that the Si 2p peak is mainly composed of SiO_2, dominating 72.29% constitution in Si chemical composition. To deeply clarify the structure of silica, SS ^{29}Si-NMR was conducted (Fig. 6), which manifests that four peaks are located at −33, −85, −101 and −110 ppm, corresponding to the structure of H_2SiN_2/H_3SiN,[41]

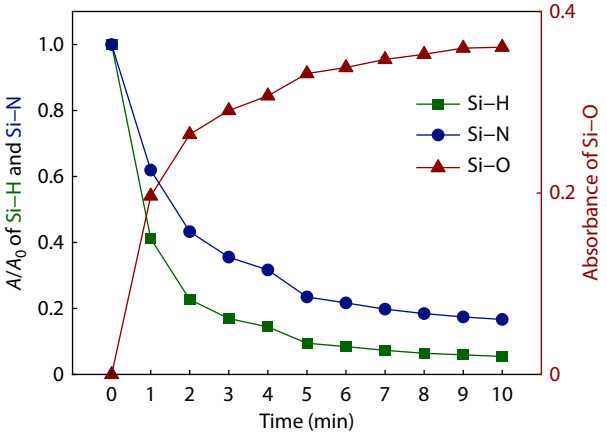

Fig. 4 Relative absorbance of Si—H and Si—N and absorbance of Si—O for different conversion time at 80 °C and 90%RH of PHPS with 5 wt% APTES.

$$\equiv Si-H + =N-H \longrightarrow \equiv Si-N= + H_2 \quad (a)$$

$$\equiv Si-NH- + H_2O \longrightarrow \equiv Si-NH_2 \quad (b)$$

Scheme 2 (a) Dehydrogenative coupling reaction of Si—H; (b) The conversion of Si—NH to Si—NH_2.

$HSiO_3/SiN_2O_2$, $SiNO_3/SiO_3OH$[42] and SiO_4.[43] The strong peaks of $SiNO_3/SiO_3OH$ and SiO_4 and the absence of H_2SiN_2/H_3SiN peaks indicate that the converted PHPS is dominated by the silica structure.

Coating Characterizations

For the application purpose, silica coating derived by PHPS with the APTES-catalytic method was investigated. The conversion from precursor polymer to silica generally causes the change in the volume of the afforded coating. Fig. 7(a) shows the variation of coating thickness and volume shrinkage with conversion time. The coating during the conversion process shows a tendency to expand slightly and then contract. The expansion at the pre-conversion stage is caused by the water absorption of the coating before the hydrolysis of Si—H and Si—N. Once the hydrolysis reaction proceeds, the water will be consumed and condensation reaction starts, which makes the coating shrink

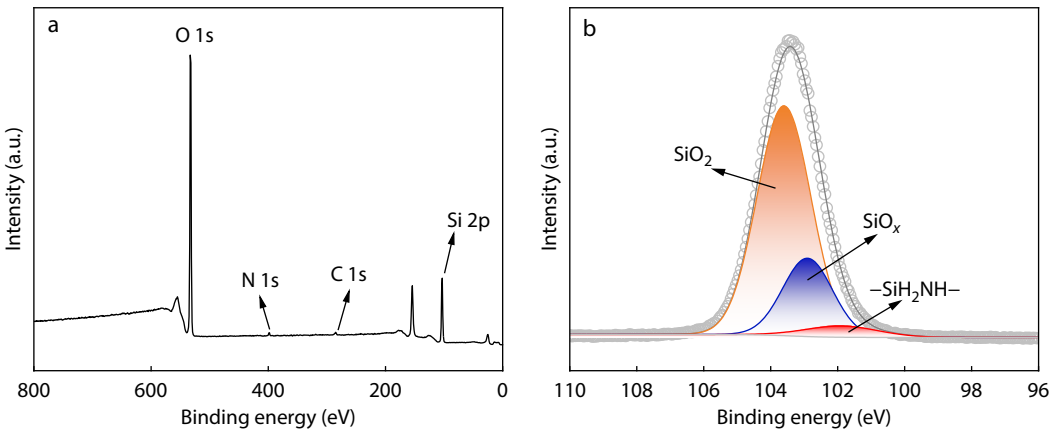

Fig. 5 (a) XPS spectrum and (b) the Si 2p spectrum of the PHPS added with 5 wt% APTES after conversion at 80 °C with 90%RH for 10 min.

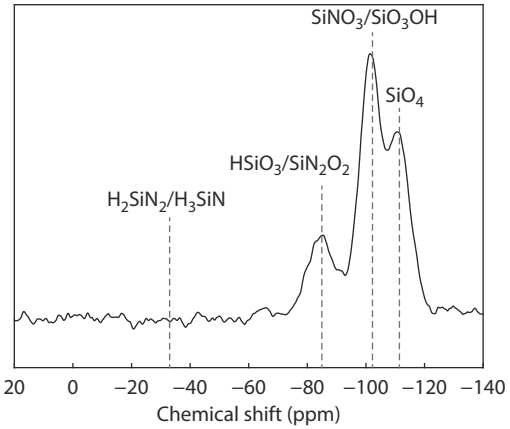

Fig. 6 The SS ^{29}Si-NMR spectrum of the PHPS added with 5 wt% APTES after conversion at 80 °C with relative humidity of 90% for 10 min.

continuously. The hydrolysis of APTES to release ethanol and following condensation reaction also leads to the shrinkage of the coating. It should be noted that the final shrinkage of the coating obtained by rapid conversion is 0.86%, which is really a low value, since the volume variant from polymer to inorganic ceramic is generally in the range of 20%–35%. We propose that up to 28.9% weight gain is the main reason for its lower volume shrinkage. Shrinkage of the film is one of its main causes of defects, so this method has the potential to suppress the generation of defects. Moreover, the low shrinkage will minimize the internal stress of the coating induced by the mismatch of volume change between coating and coated substrates.

The refractive index is directly related to the composition and free volume of the material.[44] As shown in Fig. 7(b), the refractive index of PHPS coating is up to 1.55. As the conversion proceeds, the refractive index shows a tendency to decrease, which is due to the reduction of N content. The refractive index of the final afforded coating is 1.451, slightly lower than amorphous silica (1.456).[45] We speculate that the lower shrinkage of this conversion process induces a higher free volume of the achieved coating.

The quality and the density homogeneity of the coating was further examined by the XRR technique (Fig. 8). Significant Klessig Fringes indicates the low roughness and high density homogeneity characterizations of the coating. Qualitative analysis is provided by the fitting results from the curves (Fig. 8a). The representing of the reflectivity curves produces a profile called scattering length density (SLD), which contains the summation of the scattering length and density of each atom with respect to X-ray. Since the scattering length of each atom is well known and referred in the database,[46] the density of the thin film profile can be extracted from the

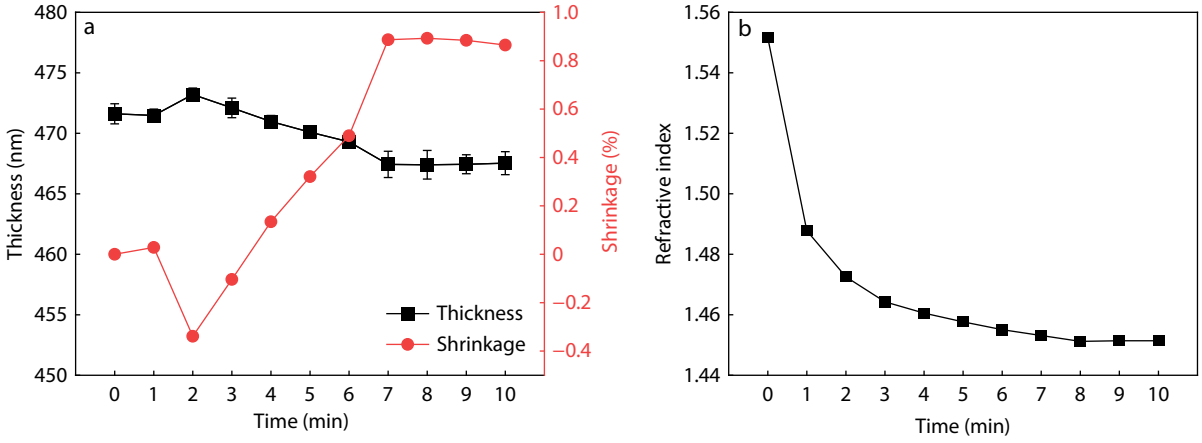

Fig. 7 Variation of (a) thickness, shrinkage and (b) refractive index of the coating with conversion time.

https://doi.org/10.1007/s10118-023-2959-6

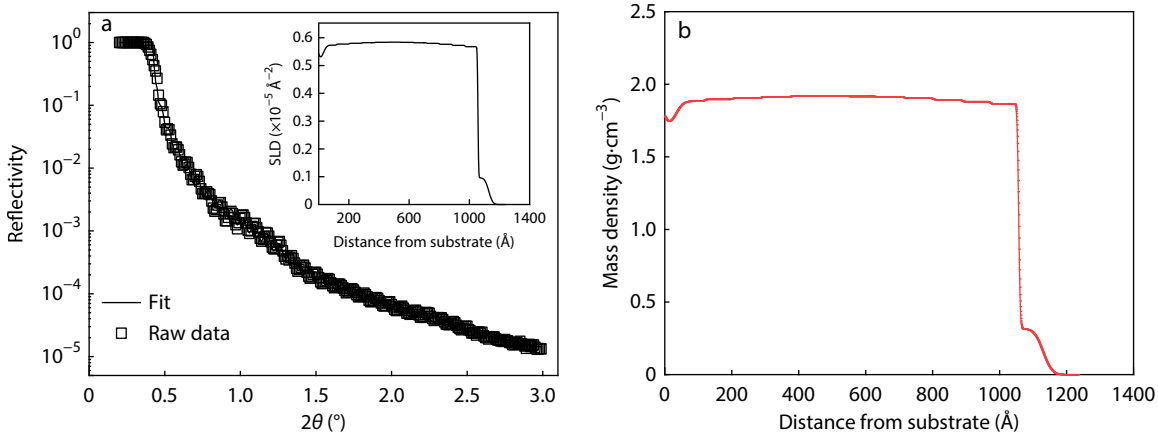

Fig. 8 (a) XRR data and fitting results for the converted coating. The dots are the raw data while the line is the representing data. The inset shows the SLD of the films as function of the coating thickness. (b) The mass density as function of distance while the density is calculated from the SLD profiles.

SLD one.

The variation of density inside the coating is produced by a consecutive various model,[47] *i.e.*, a model that slices up the coating into averaged thickness layers. Accordingly, the density of the sliced layer can be different from each other, and it is believed that this model can be more veritable to check the homogeneity of the coating. Indeed, the consecutive various model gives the best fit and yields the smallest representing factor of 0.035. The best fitting result demonstrates the whole coating thickness is 117.3 nm. Although the density parameter of each slice kept open during the fitting process, the fitted density of the main layer is almost flat and the densities tend to be equal, which manifests the high homogeneity of the prepared silica coating. Moreover, the density of the silica film is about 1.9 g/cm^3, lower than the amorphous silica density value of 2.2 g/cm^3 (Fig. 8b). In the NMR analysis result of the afforded material, except from SiO_4 (Q_4), SiO_3OH (Q_3)/$HSiN_3$ and $HSiO_3$/SiN_2O_2 dominate the structure of the afforded material, indicating the coating is composed of partial converted PHPS. Therefore, the density of the coating is lower than the amorphous silica.

The morphology of the achieved silica coating was observed by SEM and AFM. From the SEM image (Fig. 9a), it can be seen that the surface of the coating is flat and smooth without obvious defects such as holes and cracks. The roughness is only R_a=0.293 nm as measured by AFM (Fig. 9b), proving the high uniformity of afforded coating. The cross-section of the PHPS coating without catalyst is rough and inhomogeneous, exhibiting characteristics of the polymer phase (Fig. 9c). While, the silica coating from PHPS catalyzed by APTES has a flat, smooth, uniform and well-dense cross-section, which shows the characteristics of an inorganic silica phase (Fig. 9d).

The mechanical property of the coatings was measured by nanoindentation method (Fig. 10). After conversion at 80 °C with relative humidity of 90% for 10 min, the hardness of the PHPS coating without catalysis is 0.21 GPa and the elasticity modulus is 3.62 GPa. While, the silica coating from PHPS catalyzed by APTES has the hardness of 3.09 GPa and the elasticity modulus of 30.06 GPa. Actually, the hardness and modulus are remarkably higher than the polymeric materials (H<0.4 GPa, E<8 GPa).[48] Besides, pencil hardness was measured, which demonstrates that the silica coating has a pencil hardness of 9H, the highest level according to the industry standard. Therefore, the coating obtained in this work has high po-

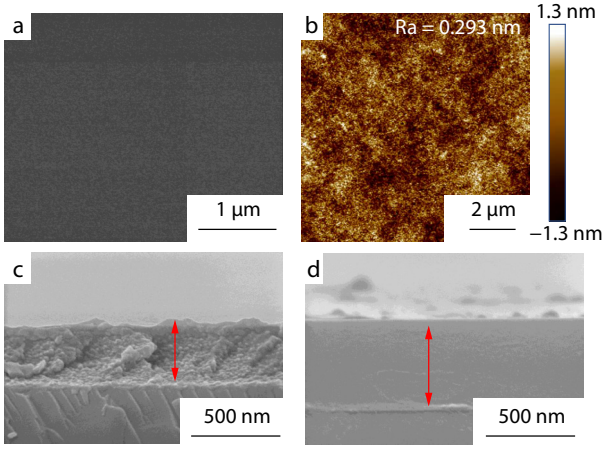

Fig. 9 (a) SEM and (b) AFM images of the surface of PHPS after catalytic conversion of APTES; SEM image of cross sections of (c) neat PHPS and (d) PHPS with 5 wt% APTES PHPS added.

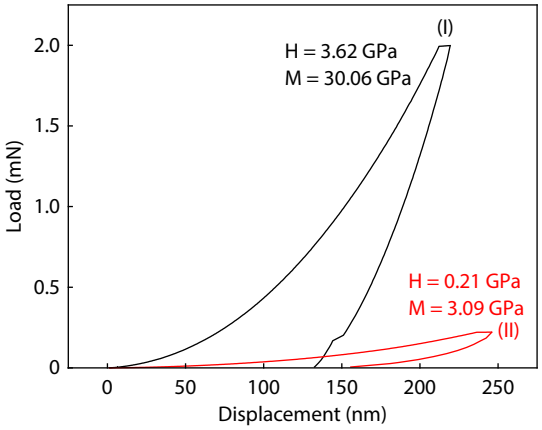

Fig. 10 Hardness (H) and modulus (M) of PHPS (I) and PHPS with 5 wt% APTES (II) at 80 °C with relative humidity of 90% for 10 min.

https://doi.org/10.1007/s10118-023-2959-6

tentials as hard protective layer for plastic, metal and other materials due to its low processed temperature and short process time.

CONCLUSIONS

In this work, we demonstrated that APTES is an effective catalyst for the conversion of PHPS to silica at low temperature. The mechanism is the hydrolysis of Si—H and Si—N in PHPS catalyzed by $-NH_2$ in APTES. The catalytic effect of APTES is enhanced with increasing temperature and humidity. PHPS can be rapidly converted to silica coating under the catalytic effect of APTES at 80 °C and 90%RH within 10 minutes. Due to the high weight gain during the conversion process, the coating has only 0.86% shrinkage and the density of the coating is 1.9 g/cm^3. The microscopic morphology indicates the coating is smooth and uniform with nanoindentation hardness of 3.09 GPa and elasticity modulus of 30.06 GPa. It is expected that the rapid process under warm condition will lead to efficient production of hard and uniform silica coatings for thermal vulnerable materials and find applications in the fields of organic encapsulation and displays.

Conflict of Interests

The authors declare no interest conflict.

Electronic Supplementary Information

Electronic supplementary information (ESI) is available free of charge in the online version of this article at http://doi.org/10.1007/s10118-023-2959-6.

ACKNOWLEDGMENTS

A portion of this work is based on the data obtained at BSRF-1W1A. The authors gratefully acknowledge the cooperation of the beamline scientists at BSRF-1W1A beamline. This work was financially supported by the National Natural Science Foundation of China (No. 21872152), Guangdong Natural Science Foundation (No. 2019A1515111028) and Xiejialin Foundation in the Institute of High Energy Physics (No. E15466U210).

REFERENCES

1 Zhang, T. T.; Zhou, M. X.; Guo, Z. Y.; Zhao, Y. B.; Han, D.; Xiu, H.; Bai, H. W.; Zhang, Q.; Fu, Q. Improving impact toughness of polylactide/ethylene-*co*-vinyl-acetate blends *via* adding fumed silica nanoparticles: effects of specific surface area-dependent interfacial selective distribution of silica. *Chinese J. Polym. Sci.* **2021**, *39*, 1040–1049.
2 Khodakarami, S.; Zhao, H. Y.; Rabbi, K. F.; Miljkovic, N. Scalable corrosion-resistant coatings for thermal applications. *ACS Appl. Mater. Interfaces* **2021**, *13*, 4519–4534.
3 Fan, L. L.; Quan, J. Y.; Zhang, H.; Yu, J. R.; Hu, Z. M.; Wang, Y. Preparation of hydrophilic UHMWPE hollow fiber membranes by chemically bounding silica nanoparticles. *Chinese J. Polym. Sci.* **2021**, *39*, 189–200.
4 Monti, M.; Dal Bianco, B.; Bertoncello, R.; Voltolina, S. New protective coatings for ancient glass: silica thin-films from perhydropolysilazane. *J. Cult. Herit.* **2008**, *9*, E143–E145.
5 Li, P. F.; Wang, D.; Zhang, Z. B.; Guo, Y. L.; Jiang, L.; Xu, C. H. Room-temperature, solution-processed SiO_x *via* photochemistry approach for highly flexible resistive switching memory. *ACS Appl. Mater. Interfaces* **2020**, *12*, 56186–56194.
6 Li, P. F.; Zhang, Y. L.; Guo, Y. L.; Jiang, L.; Zhang, Z. B.; Xu, C. H. Resistance switching behavior of a perhydropolysilazane-derived SiO_x-based memristor. *J. Phys. Chem. Lett.* **2021**, *12*, 10728–10734.
7 Back, H. S.; Kim, M. J.; Baek, J. J.; Kim, D. H.; Shin, G.; Choi, K. H.; Cho, J. H. Intense-pulsed-UV-converted perhydropolysilazane gate dielectrics for organic field-effect transistors and logic gates. *RSC Adv.* **2019**, *9*, 3169–3175.
8 Blankenburg, L.; Schrodner, M. Perhydropolysilazane derived silica for flexible transparent barrier foils using a reel-to-reel wet coating technique: single- and multilayer structures. *Surf. Coat. Technol.* **2015**, *275*, 193–206.
9 Jin, S. B.; Long, W.; Sahu, B. B.; Han, J. G.; Hori, M. Improving the gas barrier and mechanical properties of a-SiO_x films synthesized at low temperature by using high energy and hydrogen flow rate control. *J. Korean Phys. Soc.* **2015**, *66*, 1410–1415.
10 Channa, I. A.; Shah, A. A.; Rizwan, M.; Makhdoom, M. A.; Chandio, A. D.; Shar, M. A.; Mahmood, A. Process parameter optimization of a polymer derived ceramic coatings for producing ultra-high gas barrier. *Materials* **2021**, *14*, 7000.
11 Reichelt, K.; Jiang, X. The preparation of thin films by physical vapour deposition methods. *Thin Solid Films* **1990**, *191*, 91–126.
12 Mattox, D. M. Physical vapor deposition (PVD) processes. *Met. Finish.* **2000**, *98*, 410–423.
13 Boke, F.; Giner, I.; Keller, A.; Grundmeier, G.; Fischer, H. Plasma-enhanced chemical vapor deposition (PE-CVD) yields better hydrolytical stability of biocompatible SiO_x thin films on implant alumina ceramics compared to rapid thermal evaporation physical vapor deposition (PVD). *ACS Appl. Mater. Interfaces* **2016**, *8*, 17805–17816.
14 Jung, H.; Kim, W. H.; Oh, I. K.; Lee, C. W.; Lansalot-Matras, C.; Lee, S. J.; Myoung, J. M.; Lee, H. B. R.; Kim, H. Growth characteristics and electrical properties of SiO_2 thin films prepared using plasma-enhanced atomic layer deposition and chemical vapor deposition with an aminosilane precursor. *J. Mater. Sci.* **2016**, *51*, 5082–5091.
15 Aman, S. G. M; Koretomo, D.; Magari, Y.; Furuta, M. Influence of Deposition Temperature and Source Gas in PE-CVD for SiO_2 Passivation on Performance and Reliability of In-Ga-Zn-O Thin-Film Transistors. *IEEE Trans. Electr. Devices* **2018**, *65*, 3257–3263.
16 Arl, D.; Roge, V.; Adjeroud, N.; Pistillo, B. R.; Sarr, M.; Bahlawane, N.; Lenoble, D. SiO_2 thin film growth through a pure atomic layer deposition technique at room temperature. *RSC Adv.* **2020**, *10*, 18073–18081.
17 Matsuo, H.; Yamada, K. Topics on coating. Ceramic coating capable low-temperature formation using inorganic polysilazane. *Convertech* **1995**, *23*, 25–29.
18 Naganuma, Y.; Horiuchi, T.; Kato, C.; Tanaka, S. Low-temperature synthesis of silica coating on a poly(ethylene terephthalate) film from perhydropolysilazane using vacuum ultraviolet light irradiation. *Surf. Coat. Technol.* **2013**, *225*, 40–46.
19 Zhang, Z. B.; Shao, Z. H.; Luo, Y. M.; An, P. Y.; Zhang, M. Y.; Xu, C. H. Hydrophobic, transparent and hard silicon oxynitride coating from perhydropolysilazane. *Polym. Int.* **2015**, *64*, 971–978.
20 Niizeki, T.; Nagayama, S.; Hasegawa, Y.; Miyata, N.; Sahara, M.; Akutsu, K. Structural study of silica coating thin layers prepared from perhydropolysilazane: substrate dependence and water penetration structure. *Coatings* **2016**, *6*, 64.

21 Zhang, Z. B.; Wang, D.; Xiao, F. Y.; Liang, Q. Y.; Luo, Y. M.; Xu, C. H. Dense, uniform, smooth SiO_2/TiO_2 hard coatings derived from a single precursor source of tetra-nbutyl titanate modified perhydropolysilazane. *RSC Adv.* **2018**, *8*, 16746–16752.
22 Kamiya, K.; Tange, T.; Hashimoto, T.; Nasu, H.; Shimizu, H. Formation process of silica glass thin films from perhydropolysilazane. *Research Reports of the Faculty of Engineering* **2001**, *26*, 23–32.
23 Nakajima, K.; Uchiyama, H.; Kitano, T.; Kozuka, H. Conversion of solution-derived perhydropolysilazane thin films into silica in basic humid atmosphere at room temperature. *J. Am. Ceram. Soc.* **2013**, *96*, 2806–2816.
24 Zhan, Y.; Grottenmuller, R.; Li, W.; Javaid, F.; Riedel, R. Evaluation of mechanical properties and hydrophobicity of room-temperature, moisture-curable polysilazane coatings. *J. Appl. Polym. Sci.* **2021**, *138*, e50469.
25 Morlier, A.; Cros, S.; Garandet, J. P.; Alberola, N. Thin gas-barrier silica layers from perhydropolysilazane obtained through low temperature curings: a comparative study. *Thin Solid Films* **2012**, *524*, 62–66.
26 Prager, L.; Dierdorf, A.; Liebe, H.; Naumov, S.; Stojanovic, S.; Heller, R.; Wennrich, L.; Buchmeiser, M. R. Conversion of perhydropolysilazane into a SiO_x network triggered by vacuum ultraviolet irradiation: access to flexible, transparent barrier coatings. *Chem. Eur. J.* **2007**, *13*, 8522–8529.
27 Kubo, T.; Tadaoka, E.; Kozuka, H. Preparation of hot water-resistant silica thin films from polysilazane solution at room temperature. *J. Sol-gel Sci. Technol.* **2004**, *31*, 257–261.
28 Kubo, T.; Kozuka, H. Conversion of perhydropolysilazane-to-silica thin films by exposure to vapor from aqueous ammonia at room temperature. *J. Ceram. Soc. JAPAN* **2006**, *114*, 517–523.
29 Kozuka, H.; Fujita, M.; Tamoto, S. Polysilazane as the source of silica: the formation of dense silica coatings at room temperature and the new route to organic-inorganic hybrids. *J. Sol-gel Sci. Technol.* **2008**, *48*, 148–155.
30 Lee, J. S.; Oh, J. H.; Moon, S. W.; Sul, W. S.; Kim S. D. A Technique for Converting Perhydropolysilazane to SiO_x at Low Temperature. *Electrochem. Solid ST.* **2010**, *13*, H23–H25.
31 Jung, S. H.; Lee, J. S.; Oh, J. H.; Moon, S. W.; Kim, S. D. Method of low-temperature conversion of pehydropolysilazane into amorphous SiO_x in aqueous solutions. *Jpn. J. Appl. Phys.* **2010**, *49*, 111505.
32 Bauer, F.; Decker, U.; Dierdorf, A.; Ernst, H.; Heller, R.; Liebe, H.; Mehnert, R. Preparation of moisture curable polysilazane coatings. Part I. Elucidation of low temperature curing kinetics by FT-IR spectroscopy. *Prog. Org. Coat.* **2005**, *53*, 183–190.
33 Je, S. Y.; Son, B. G.; Kim, H. G.; Park, M. Y.; Do, L. M.; Choi, R.; Jeong, J. K. Solution-processable $LaZrO_x/SiO_2$ gate dielectric at low temperature of 180 °C for high-performance metal oxide field-effect transistors. *ACS Appl. Mater. Interfaces* **2014**, *6*, 18693–18703.
34 Oliver, W. C.; Pharr, G. M. An improved technique for determining hardness and elastic modulus using load and displacement sensing indentation experiments. *J. Mater. Res.* **1992**, *7*, 1564–1583.
35 Xu, D. S.; Sun, L.; Li, H. L.; Zhang, L.; Guo, G. L.; Zhao, X. S.; Gui, L. L. Hydrolysis and silanization of the hydrosilicon surface of freshly prepared porous silicon by an amine catalytic reaction. *New J. Chem.* **2003**, *27*, 300–306.
36 Perera, D. Y.; Selier, P. Water transport in organic coatings. *Prog. Org. Coat.* **1973**, *2*, 57–80.
37 Chen, Q.; Zhang, X. S.; Wang, F. Experimental study of thermal diffusion enhanced vapor transfer performance with perhydropolysilazane-derived silica (PDS) coating membranes in air dehumidification process. *Int. J. Refrig.* **2021**, *122*, 21–32.
38 Gunthner, M.; Wang, K.; Bordia, R. K.; Motz, G. Conversion behaviour and resulting mechanical properties of polysilazane-based coatings. *J. Eur. Ceram. Soc.* **2012**, *32*, 1883–1892.
39 Muller, S.; de Hazan, Y.; Penner, D. Effect of temperature, humidity and aminoalkoxysilane additive on the low temperature curing of polyorganosilazane coatings studied by IR spectroscopy, gravimetric and evolved gas analysis. *Prog. Org. Coat.* **2016**, *97*, 133–145.
40 Kang, Y. H.; Min, B. K.; Kim, S. K.; Bae, G.; Song, W.; Lee, C.; Cho, S. Y.; An, K. S. Proton conducting perhydropolysilazane-derived gate dielectric for solution-processed metal oxide-based thin-film transistors. *ACS Appl. Mater. Interfaces* **2020**, *12*, 15396–15405.
41 Iwamoto, Y.; Kikuta, K. I.; Hirano, S. I. Si_3N_4-TiN-Y_2O_3 ceramics derived from chemically modified perhydropolysilazane. *J. Mater. Res.* **1999**, *14*, 4294–4301.
42 Lin, R. Y.; Carlstrom, G.; Pham, Q. D.; Anderson, M. W.; Topgaard, D.; Edler, K. J.; Alfredsson, V. Kinetic influence of siliceous reactions on structure formation of mesoporous silica formed *via* the co-structure directing agent route. *J. Phys. Chem. C* **2016**, *120*, 3814–3821.
43 Miloskovska, E.; Hansen, M. R.; Friedrich, C.; Hristova-Bogaerds, D.; van Duin, M.; de With, G. *In situ* silica nanoparticle formation in a rubber matrix monitored *via* real-time SAXS and solid-state NMR spectroscopy. *Macromolecules* **2014,** *47*, 5174-5185.
44 Yang, C. C.; Chen, W. C. The structures and properties of hydrogen silsesquioxane (HSQ) films produced by thermal curing. *J. Mater. Chem.* **2002**, *12*, 1138–1141.
45 Nikitin, T.; Velagapudi, R.; Sainio, J.; Lahtinen, J.; Rasanen, M.; Novikov, S.; Khriachtchev, L. Optical and structural properties of SiO_x films grown by molecular beam deposition: effect of the Si concentration and annealing temperature. *J. Appl. Phys.* **2012**, *112*, 094316.
46 https://henke.lbl.gov/optical_constants/asf.html.
47 Wang, L. M.; Li, Q. D.; Liu, S. J.; Cao, Z. X.; Cai, Y. P.; Jiao, X. C.; Lai, H. J.; Xie, W. G.; Zhan, X. Z.; Zhu, T. Quantitative determination of the vertical segregation and molecular ordering of PBDB-T/ITIC blend films with solvent additives. *ACS Appl. Mater. Interfaces* **2020**, *12*, 24165–24173.
48 Briscoe, B. J.; Fiori, L.; Pelillo, E. Nano-indentation of polymeric surfaces. *J. Phys. D* **1998**, *31*, 2395.

https://doi.org/10.1007/s10118-023-2959-6